

Spherical Waves, Light Propagation, and Partial Coherence

Grover Swartzlander, March 2023

A. Rayleigh-Sommerfeld

The Rayleigh-Sommerfeld Diffraction Integral, expressed,

$$E(x', y', z) = \frac{z}{i\lambda} \iint \frac{E(x, y, 0)}{(x - x')^2 + (y - y')^2 + z^2} e^{ik\sqrt{(x-x')^2 + (y-y')^2 + z^2}} dx dy \quad (1)$$

describes that the field at z owing to interfering spherical waves having sources at the plane $z = 0$. For a single points source at $z = 0$, located at the position $(x, y) = (a, b)$ such that $E(x, y, 0) = A\delta(x - a)\delta(y - b)$, Eq. 1 provides

$$\begin{aligned} E(x', y', z) &= \frac{Az}{i\lambda} \iint \frac{\delta(x - a)\delta(y - b)}{(x - x')^2 + (y - y')^2 + z^2} e^{ik\sqrt{(x-x')^2 + (y-y')^2 + z^2}} dx dy \\ &= \frac{Az}{i\lambda} e^{ik\sqrt{(a-x')^2 + (b-y')^2 + z^2}} / (a - x')^2 + (b - y')^2 + z^2 \end{aligned} \quad (2)$$

For a distribution of N sources at $z = 0$ emitting spherical waves of strength A_j at the points (a_j, b_j) , the net field at the distance z is given by the linear superposition:

$$\begin{aligned} E(x', y', z) &= \frac{z}{i\lambda} \sum_{j=1}^N A_j e^{ik\sqrt{(a_j-x')^2 + (b_j-y')^2 + z^2}} / (a_j - x')^2 + (b_j - y')^2 + z^2 \\ &\equiv |E(x', y', z)| \exp(i\Phi(x', y', z)) \end{aligned} \quad (3)$$

Momentarily consider the case where $z^2 \gg (a_j - x')^2 + (b_j - y')^2$ such that the phase terms in Eq. 3 may be expressed

$$\begin{aligned} \Phi_j &= k\sqrt{(a_j - x')^2 + (b_j - y')^2 + z^2} \approx kz + k(a_j - x')^2/2z + k(b_j - y')^2/2z \\ &= k\left(z + (x'^2 + y'^2)/2z\right) + k(a_j^2 + b_j^2)/2z - ka_jx'/z - kb_jy'/z \\ &\equiv \Phi_0(x', y', z) + \Delta\Phi_j(x', y', a_j, b_j, z) \end{aligned} \quad (4)$$

where Φ_0 is the small angle approximation of the exact expression $\Phi_0 = k\sqrt{x'^2 + y'^2 + z^2}$. We observe that Φ_0 is independent of the source points (a_j, b_j) , and thus it represents a common phase for all source points. Below we shall examine both the net phase Φ (see Eq. 3) and the phase difference $\Delta\Phi = \Phi - \Phi_0$ where we will use the exact expression: $\Phi_0 = k\sqrt{x'^2 + y'^2 + z^2}$.

The net phase Φ of the electric field (see Eq. 3) is found by taking the arctangent of the following expression:

$$\tan \Phi = \text{IM}[E(x', y', z)] / \text{RE}[E(x', y', z)] \quad (5)$$

The phase different $\Delta\Phi$ corresponds to the phase of the modified field $E(x', y', z) \exp(-i\Phi_0)$, where $\Phi_0 = k\sqrt{x'^2 + y'^2 + z^2}$. To determine $\Delta\Phi$ we take the arctangent of

$$\tan(\Delta\Phi) = \text{IM}[E(x', y', z) \exp(-i\Phi_0)] / \text{RE}[E(x', y', z) \exp(-i\Phi_0)] \quad (6)$$

Note: You must use a function such as *arctan2(y,x)* to numerically compute the correct phase.

Example: Two Point Sources

Let's consider two point sources emitting light at $\lambda = 1 \text{ [\mu m]}$ from the points $(a, 0)$ and $(-a, 0)$ where $a = 50 \text{ [\mu m]}$, propagating to various distances, z . The characteristic diffraction distance of this system is $Z_0 = \pi a^2 / \lambda \approx 8 \text{ [mm]}$.

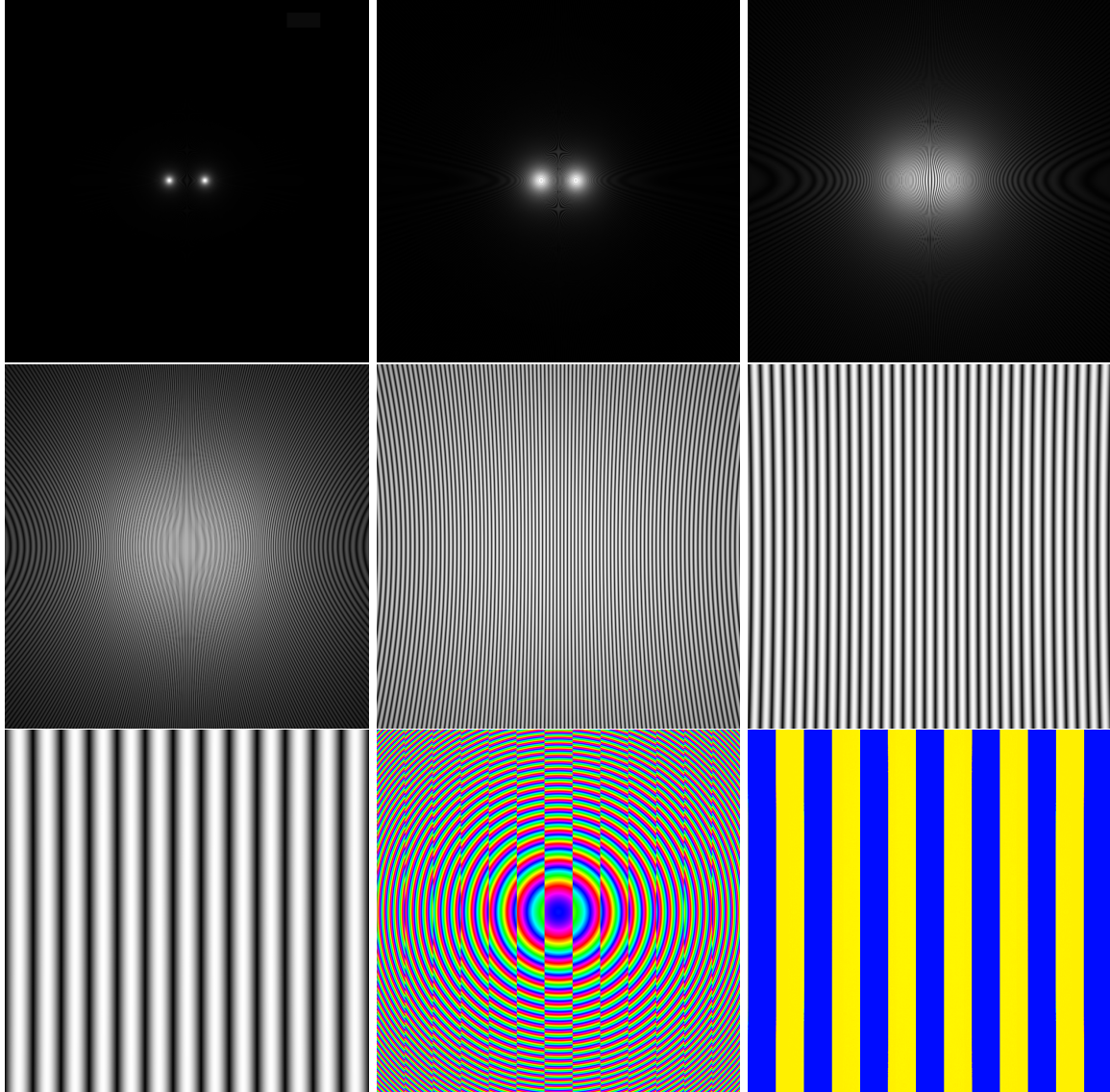


Figure 1: Distributions in the x', y' plane at various distances z for two point sources separated by $2a = 100 \text{ [\mu m]}$, and for $\lambda = 1 \text{ [\mu m]}$. Image dimensions: $1024\lambda \times 1024\lambda$. Top row (left to right): $|E(x', y', z)|$ at $z = 10, 50, 100 \text{ [\mu m]}$. Middle row (left to right): $|E(x', y', z)|$ at $300, 1000, 3000 \text{ [\mu m]}$. Bottom row (left to right) at $z = Z_0 = 7.854 \text{ [mm]}$: $|E(x', y', z)|$, Phase Φ , and $\Delta\Phi = \Phi - \Phi_0$. The phase difference between adjacent stripes in $\Delta\Phi$ is π .

Example: Five Point Sources

Consider five point sources emitting light for the wavelength $\lambda = 1 \text{ [\mu m]}$ from the equidistant points on a circle of radius $a = 50 \text{ [\mu m]}$. Let us examine the field amplitude and phase at the distance $z = Z_0 = \pi a^2 / \lambda$. As in Fig. 1, there is a significant difference between the net phase Φ and the phase with the common wavefront curvature removed, i.e., $\Delta\Phi = \Phi - \Phi_0$.

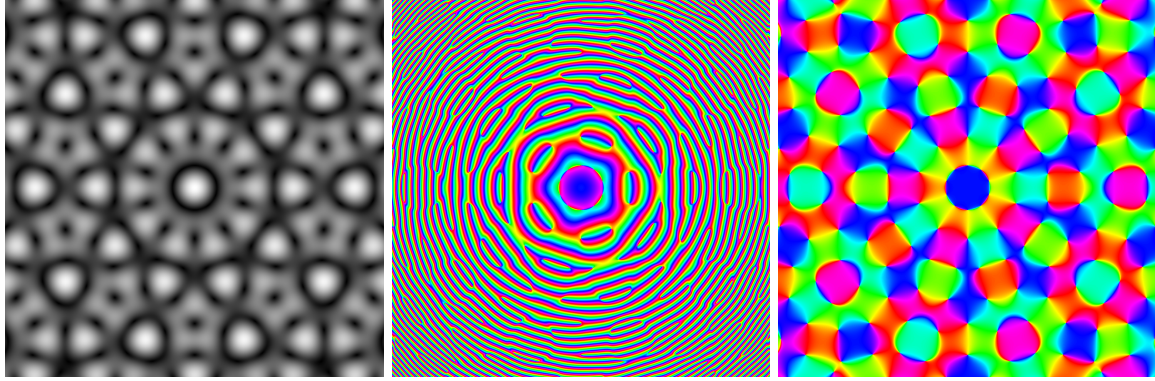


Figure 2: Distributions in the x', y' plane at $z = Z_0 = 7.854 \text{ [\mu m]}$. Five point sources uniformly distributed on a circle of radius $a = 50 \text{ [\mu m]}$. Wavelength: $\lambda = 1 \text{ [\mu m]}$. Image dimensions: $1024\lambda \times 1024\lambda$. Left to right: $|E|$, Φ , and $\Phi - \Phi_0$.

B. Coherence, Speckle, and Incoherence

We have seen above that the propagation of light may be described by the interference between multiple point source of light. Associated with each source point in Eq. 3 is the factor A_j which describes both the strength of emitted light and the phase. Let us therefore write $A_j = |A_j| \exp(i\phi_j)$. If the values of phase terms are fixed in time, then the field is said to be coherent. (This statement is true even in the case where the phases have random values.) On the other hand, if ϕ_j varies randomly in time, then the field is said to be partially coherent. The time-averaged irradiance of a fully incoherent beam will exhibit no interference phenomena, whereas a partially incoherent beam will exhibit partial interference. Coherence can be measured using interference techniques and is therefore related to contrast. Note that measures of coherence requires time averaging over the exposure time of the detector. Another key point in understanding coherence is that at any instant of time (i.e., before time averaging), interference always occurs. This means that we may always use Eq. 3 to describe the net instantaneous electric field, even if the phases ϕ_j are randomly related to each other. In this example let us compare two cases: one with $\phi_j = 0$, and one with ϕ_j equal to a random value between $-\pi$ and π .

Two different types of interference are observed in Fig. 3. The case $\phi_j = 0$ (top row) produces a distinct central bright spot in $|E(x', y', z)|$. In contrast, the random distribution of the values of ϕ_j (bottom row) produces a “speckle” field having many bright spots in $|E(x', y', z)|$. Notice that in both cases the spots are roughly the same size. This similarity is related to the fact that the distribution of point sources for the two cases are constrained to the same size, $a = 50 \text{ [\mu m]}$. Speckle may be readily observed when a coherent laser beam scatters from a rough surface. Both the cases shown in Fig. 3 describe coherent light.

To observe incoherent phenomena we must (1) vary the values of ϕ_j randomly in time, and (2) time average. This process is depicted in Fig. 4. In this numerical example time-averaging is represented by summing the irradiance distributions of M different speckle images. The position of the N point sources is not changed when computing different speckle images; however, the phase of each point source is randomly varied. The degree of coherence is related to contrast of the image, $C = (I_{max} - I_{min}) / (I_{max} + I_{min})$. For the irradiance profiles depicted in Fig. 3, $C = 1$ and the beam is therefore perfectly coherent. In Fig. 4 however, the “measured” irradiance profiles have decreasing values of contrast, and thus the beams are said to be partially coherent, tending toward perfect incoherence as $C \rightarrow 0$.

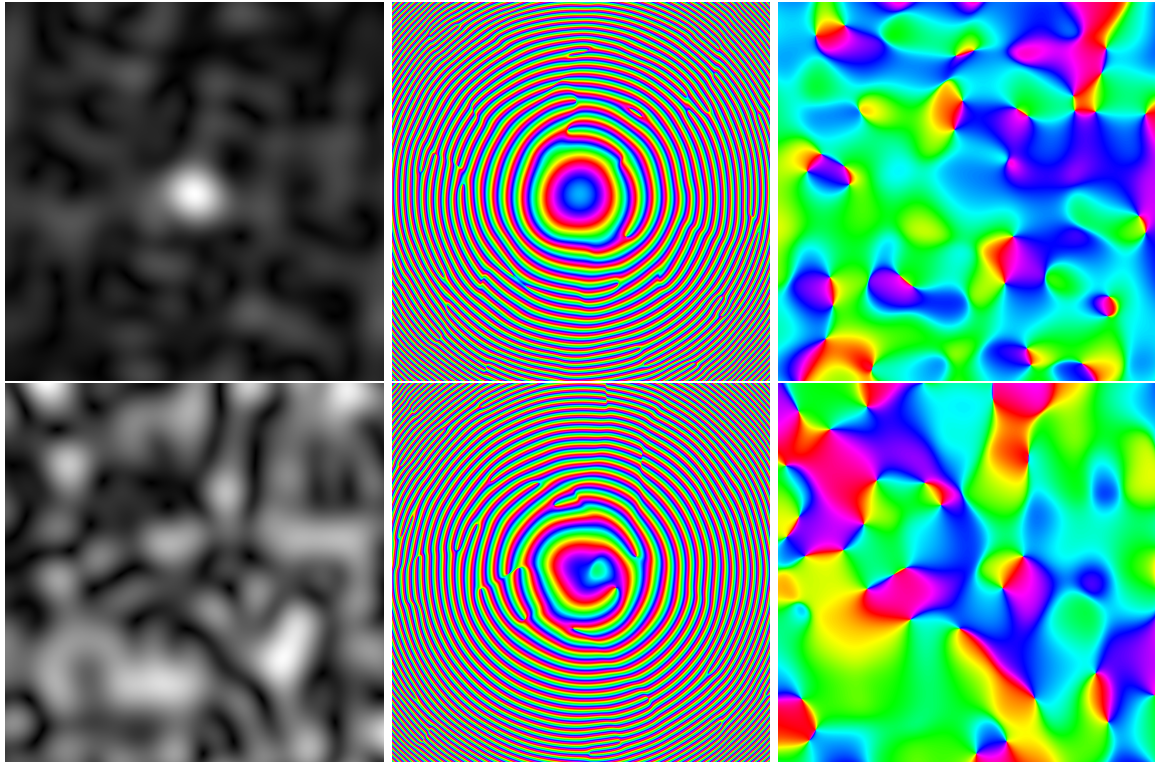


Figure 3: Distributions in the x', y' plane at $z = Z_0 = 7.854 \text{ } [\mu\text{m}]$. Fifty point sources randomly distributed within a circle of radius $a = 50 \text{ } [\mu\text{m}]$. Wavelength: $\lambda = 1 \text{ } [\mu\text{m}]$. Image dimensions: $1024\lambda \times 1024\lambda$. Top row (left to right): $|E|$, Φ , and $\Phi - \Phi_0$ for the case $\phi_j = 0$. Bottom row (left to right): $|E|$, Φ , and $\Phi - \Phi_0$ for ϕ_j equal to random numbers between $-\pi$ and π .

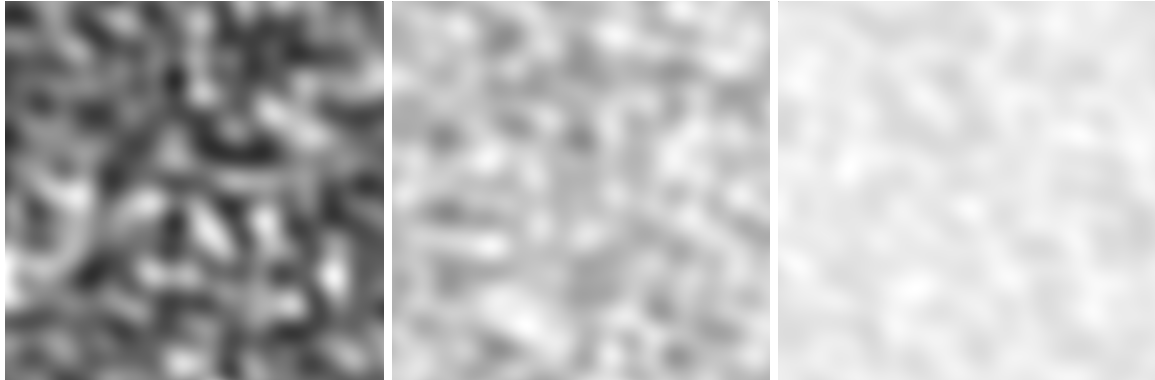


Figure 4: Distributions in the x', y' plane at $z = Z_0 = 7.854 \text{ } [\mu\text{m}]$. Time-averaged irradiance $\langle |E|^2 \rangle$ over M random instances of speckle patterns. In each instance the positions of the $N = 50$ points sources do not change, but the phase of each source ϕ_j varies from one instance to the next. Left to right: $M=10, 100, 1000$. The irradiance contrast decreases and thus the degree of coherence decreases as the value of M increases.

C. Field Flattening, Lens Transformation

In the laboratory a lens (or other elements) may be used to remove the common phase Φ_0 from the electric field. This flattens the wave front at the exit face of the lens, thereby collimating the beam. However the collimation is not perfect for a spherical lens, as illustrated below. The wavefront error is approximately given by $\Delta\phi = -kx^4/4f^3$. This can be expressed as the number of waves of wavefront error $\Delta\phi/2\pi = -x^4/4\lambda f^3$. For example, to achieve a wavefront error of a hundredth of a wave ($\Delta\phi/2\pi = 1/100$), the lens must be stopped down to a radius less than $(4\lambda f^3/100)^{1/4}$. For a lens of focal length $f = 1 \text{ [m]}$ and a source of wavelength $\lambda = 10^{-6} \text{ [m]}$, this corresponds to an aperture of diameter 2.8 [cm] , resulting in an f-number of this system is $f^\# = 35$. An example of the input and output wave front curvatures of a collimating spherical lens is depicted in Fig. 6

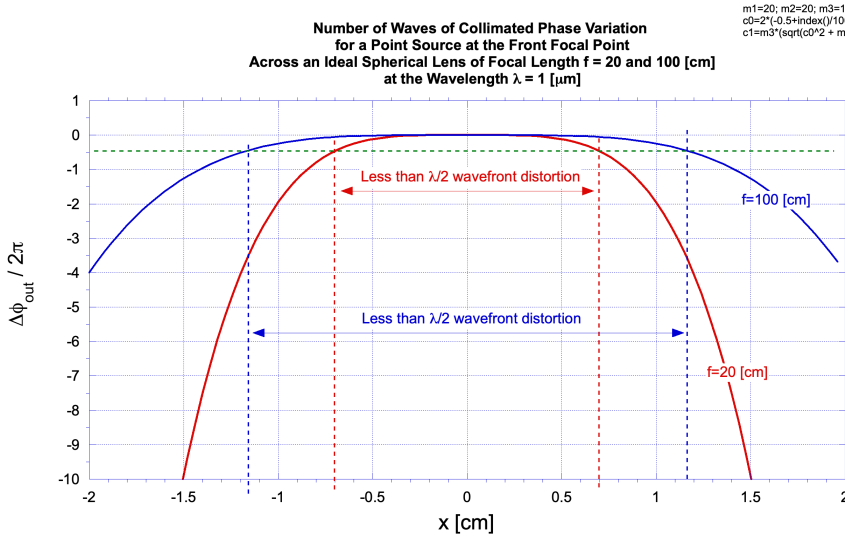
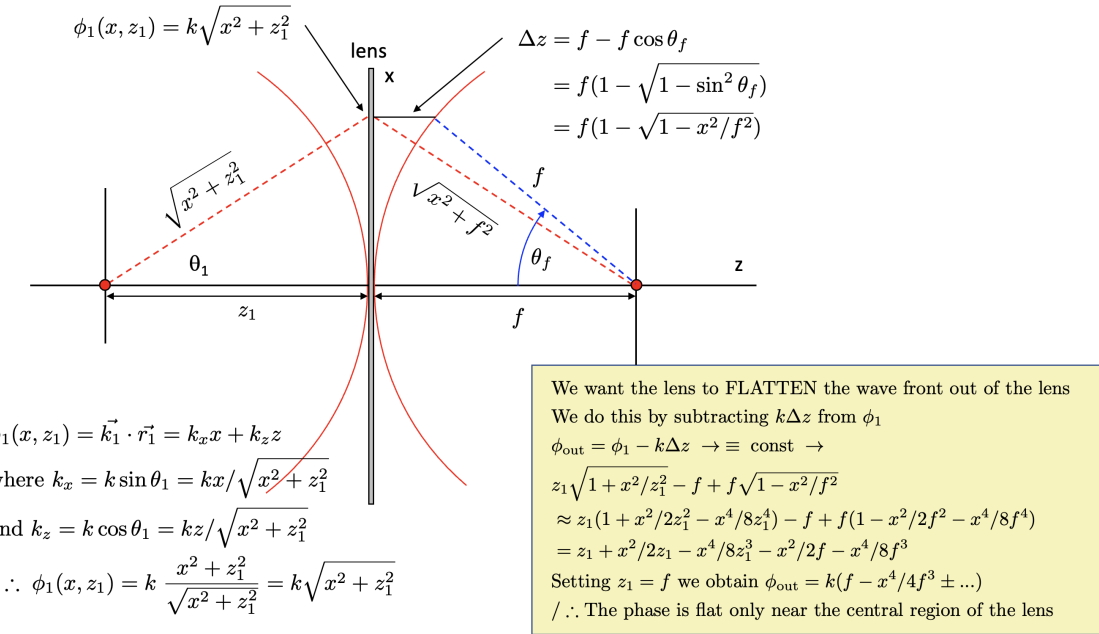


Figure 5: A spherical lens of focal length f approximately flattens the transmitted wave front when a point source is placed at the front focal point $z_1 = f$. The distance at which the wave front is flat (e.g., to within less than half a wave) increases as the focal length increases.

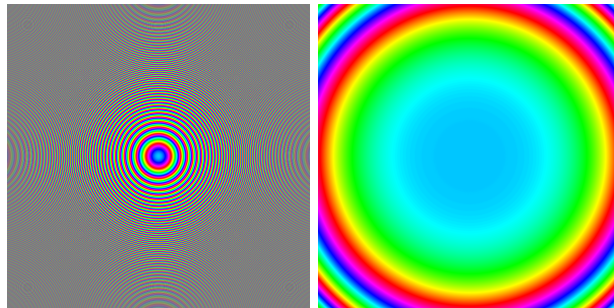


Figure 6: Left: Phase at the input face of a lens owing to a single on-axis point source at the front focal point. Right: Phase at the output face of the lens depicting a flattened phase in the central region.

D. Optical field in the back focal plane of a lens

The Rayleigh-Sommerfeld diffraction integral (see Eq. 1) reduces to the Fresnel integral by replacing $z/((x-x')^2 + (y-y')^2 + z^2)$ with the approximate expression $1/z$, and making use of the Taylor series expansion for the radical in the exponent $\sqrt{(x-x')^2 + (y-y')^2 + z^2} \approx z + (x-x')^2/2z + (y-y')^2/2z$ whereupon

$$E'(x', y', z) \approx \frac{e^{ikz}}{i\lambda z} e^{ik(x'^2+y'^2)/2z} \iint E(x, y, 0) e^{ik(x^2+y^2)/2z} e^{ikxx'/z} e^{ikyy'/z} dx dy \quad (7)$$

The Fresnel integral is particularly useful for describing the approximate electric field in the back focal plane of a lens, $E'(x', y', z = f)$, given the electric field at the input face of a lens, $E(x, y, z = 0)$ and the lens aperture function $A_{\text{lens}}(x, y)$. As suggested in the top of Fig. 5, the phase introduced by a lens is given by

$$\begin{aligned} \phi_{\text{lens}} &= -k\Delta z = -kf(1 - \sqrt{1 - x^2/f^2 - y^2/2f}) = -kf(1 - (1 - (x^2 + y^2)/2f^2 - (x^4 + y^4)/8f^4) - \dots) \\ &\approx -k(x^2/2f + y^2/2f) \end{aligned} \quad (8)$$

$$\begin{aligned} E'(x', y', f) &= \frac{e^{ikf}}{i\lambda f} e^{ik(x'^2+y'^2)/2f} \iint E(x, y, 0) A_{\text{lens}}(x, y) e^{i\phi_{\text{lens}}} e^{ik(x^2+y^2)/2f} e^{ikxx'/f} e^{ikyy'/f} dx dy \\ &= \frac{e^{ikf}}{i\lambda f} e^{if(k_x^2+k_y^2)/2k} \iint E(x, y, 0) A_{\text{lens}}(x, y) e^{ik_x x} e^{ik_y y} dx dy \end{aligned} \quad (9)$$

where $k_x = kx'/f$ and $k_y = ky'/f$, and the integral on the right hand side of Eq. 9 is simply the Fourier transform of the incident field and the aperture function.

Example: Plane wave at a circular lens aperture.

If $A(x, y)$ is described by a circular aperture of radius R and the incident field is given by $E(x, y, 0) = 1$, then Eq. 9 may be solved either analytically or numerically. Let us examine the numerical solution by making use of the fast-Fourier transform algorithm.

We expect the solution to be a Bessel-sinc function having its first zero at a radial distance $q_0 = 1.22\lambda f/D$, or equivalently, at an angle $\theta_0 = 1.22\lambda/D$. To verify whether this zero point appears at the correct location in our numerical grid, let's first consider how the grid corresponds to real and k space.

Let's choose a grid spacing $\Delta x = 10\lambda$ and a square grid of side $N = 2048$. Placing the origin (or the intersection with the optical axis) at the center of the grid, the physical extend of the grid ranges from $-L$ to L , where $L = N\Delta x/2$. In k space each pixel corresponds to an increment $\Delta k_x = \pi/L = 2\pi/N\Delta x = 2\pi/10N\lambda$. Therefore the first zero of the Bessel-sinc pattern should appear $k\theta_0/\Delta k_x$ pixels from the optical axis. To solve this we must first establish the value of D . Let $D = 2\sqrt{N/\pi}\Delta x$.

$$\frac{k\theta_0}{\Delta k_x} = \frac{2\pi}{\lambda} \frac{1.22\lambda}{2\sqrt{N/\pi} 10\lambda} \frac{10N\lambda}{2\pi} = \frac{1.22N}{2\sqrt{N/\pi}} = 1.08\sqrt{N} = 48.9 \text{ [pixels]} \quad (10)$$

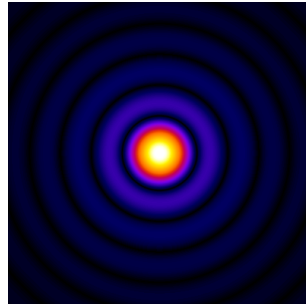


Figure 7: Fourier transform of a circular aperture function (cropped from 2048×2048 to 400×400 pixels). For an aperture radius of $\sqrt{N/\pi}$ pixels the first zero of the Bessel-Sinc function appears at $1.08\sqrt{N}$ pixels.

Example: Two resolved point sources.

A classic example depicting the comparison between coherent and incoherent light is the two point-source problem. When the two sources are barely resolvable, as depicted in Fig. 8, the coherent image depicts pronounced interference between two in-phase point sources. In this example, light has propagated a finite distance to the lens, producing the field $E_1 + E_2$ at the input face of the lens. The irradiance in the focal plane is proportional to the squared magnitude of the Fourier transform: $|\text{FT}[E_1 + E_2]|^2$. The left and middle images in Fig. 8 illustrate how interference is affected by the relative phase of the two mutually coherent sources. When the same two sources are incoherently related, the time-averaged irradiance in the focal plane may be expressed as the sum of two terms: $|\text{FT}[E_1]|^2 + |\text{FT}[E_2]|^2$. Interference is not observed in this case. Note that the focal plane distributions in Fig. 8 correspond to defocused images because the sources were not placed at infinity from the lens.

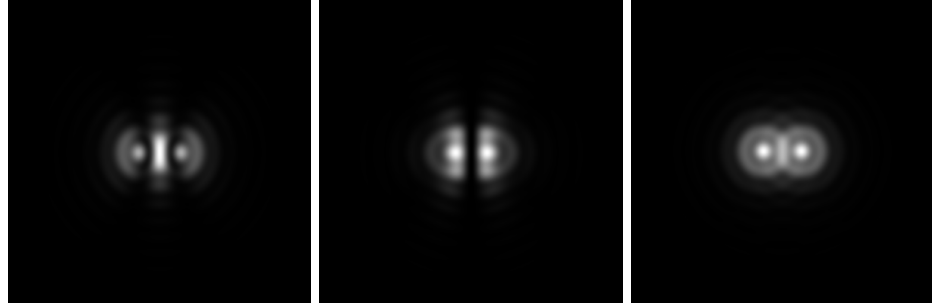


Figure 8: Left: Image (defocused) of two coherent in-phase point sources in the focal plane: $|\text{FT}[E_1 + E_2]|^2$. Middle: Same, but for out-of-phase point sources, $|\text{FT}[E_1 + E_2 \exp(i\pi)]|^2$. Right: Image (defocused) of two incoherent point sources, $|\text{FT}[E_1]|^2 + |\text{FT}[E_2]|^2$. Both sources are 205 [mm] from the lens (not at infinity), separated by 0.511 [mm] in the source plane. The in-focus images appear in the image plane (not shown), not in the focal plane. Wavelength: $\lambda = 1 [\mu\text{m}]$.